

# Light scattering analysis by a particle of extreme shape via discrete sources method

Elena Eremina<sup>a,\*</sup>, Thomas Wriedt<sup>b</sup>

<sup>a</sup>*Institut für Werkstofftechnik, Universität Bremen, Badgasteiner Str. 3, 28359 Bremen, Germany*

<sup>b</sup>*Institut für Werkstofftechnik, Badgasteiner Str. 3, 28359 Bremen, Germany*

---

## Abstract

The discrete sources method (DSM) is applied to the analysis of light scattering by particles of extreme shapes. Such investigations are needed in many scientific areas, such as particle characterization, investigation of scattering properties of atmospheric particles, interstellar dust and ice crystals, biological cells and others. Different methods have been applied to treat the problem, but usually their range of applicability is restricted to quite low aspect ratios. In this paper, a new approach of DSM to light scattering by highly elongated and flat particles is presented. The algorithm described in this paper allows to compute light scattering by elongated particles with aspect ratios up to 1:50 and for flat particles with aspect ratios till 20:1. The results obtained using DSM also allow to compare common shapes, like elongated spheroid and cylinder or flat spheroid and disk-sphere.

© 2004 Elsevier Ltd. All rights reserved.

*Keywords:* Discrete sources method; Elongated particle; Flat particle

---

## 1. Introduction

The problem of light scattering by particles of extreme shape is of great interest in recent years. According to the shape of particles the problem can be divided into two: highly elongated shapes and flat shapes. The investigation of elongated particles is needed in different areas of science. Due

---

\*Corresponding author. Tel.: +49-421-218-3583; fax: +49-421-218-5378.

*E-mail address:* [eremina@iwt.uni-bremen.de](mailto:eremina@iwt.uni-bremen.de) (E. Eremina).

to the development of new isolating materials used in buildings and other high-temperature applications interest in airborne fibers increases. Such fibers can cause serious health hazards, especially lung cancer. The health hazard of airborne respirable fibers mainly depends on their geometries, especially the aspect ratio: the higher the ratio the more dangerous the fibers are classified. In atmospheric science attention is concentrated on ice crystals, which often have an elongated shape. In astrophysics the optical properties of cosmic dust grains which are detected in various astronomical objects are very important. In optical particle characterization investigations of light scattering are needed to design instruments to measure the size of particles. Owing to this great interest in light scattering by highly elongated particles, many methods were applied to such investigations: T-Matrix method, generalized multipole techniques (GMT) [1], multiple multipole program (MMP) [2], null field method with discrete sources [3]. But usually the range of their validity does not achieve an aspect ratio higher than 1:20.

Investigation of light scattering by flat objects is needed for example in biology for the interpretation of red blood cells investigations or in analysis of silicon wafers surface. Thus, light scattering by extreme-shaped particles is of great interest in many scientific branches. But in this case usually all the methods are restricted to the aspect ratio not more than 10:1.

In this case using of discrete sources method (DSM) seems to be very reasonable. DSM is one of the most powerful tools for studying light scattering from any axial symmetric object. High aspect ratio in case of flat particle can be achieved due to free choice of discrete sources (DS) support. Besides DSM allows to calculate an a-posterior surface residual to estimate numerical result error. In this paper renewed scheme of DSM is described. We paid attention to detailed description of the numerical algorithm. The simulation results for prolate particles with an aspect ratio of 1:50 and for flat particles with an aspect ratio of 20:1 are also given.

## 2. Theory

Let us start with the mathematical statement of the scattering problem. We will consider scattering in an isotropic homogeneous medium  $R^3$  of an electromagnetic wave by a local homogeneous penetrable obstacle  $D_i$  with the smooth boundary  $\partial D$ . We use a spherical coordinate system  $(\rho, \theta, \varphi)$ ,  $\theta_0$  is the incident angle of a plane wave. We assume the time dependence to be  $\exp(j\omega t)$ . Scattering is described by the electromagnetic fields  $\{\mathbf{E}_{e,i}, \mathbf{H}_{e,i}\}$  satisfying Maxwell equations

$$\begin{aligned} \nabla \times \mathbf{H}_{e,i} &= jk\varepsilon_{e,i}\mathbf{E}_{e,i} \\ \nabla \times \mathbf{E}_{e,i} &= -jk\mu_{e,i}\mathbf{H}_{e,i} \end{aligned} \quad \text{in } D_{e,i}, \quad D_e := R^3/\bar{D}_i, \quad (1)$$

the boundary conditions enforced on the particle surface

$$\begin{aligned} \mathbf{n}_p \times (\mathbf{E}_i(P) - \mathbf{E}_e(P)) &= \mathbf{n}_p \times \mathbf{E}^0(P), \\ \mathbf{n}_p \times (\mathbf{H}_i(P) - \mathbf{H}_e(P)) &= \mathbf{n}_p \times \mathbf{H}^0(P), \end{aligned} \quad P \in \partial D, \quad (2)$$

and Silver–Muller radiation condition at infinity

$$\lim_{r \rightarrow \infty} \left( \sqrt{\varepsilon_e} \mathbf{E}_e \times \frac{\mathbf{r}}{r} - \sqrt{\mu_e} \mathbf{H}_e \right) = 0, \quad r = |M| \rightarrow \infty. \quad (3)$$

Here  $\{\mathbf{E}^0, \mathbf{H}^0\}$  is an exciting field,  $\{\mathbf{E}_e, \mathbf{H}_e\}$  is the scattered field,  $\mathbf{n}_p$  is the unit outward normal to  $\partial D$ , index e belongs to the external domain  $D_e$  and i to the domain inside the particle  $D_i$ ,  $\varepsilon_{e,i}$  is the permittivity,  $\mu_{e,i}$  is the permeability of media,  $\text{Im } \varepsilon_e, \mu_e = 0$ ,  $\text{Im } \varepsilon_i, \mu_i \leq 0$ . The boundary value scattering problem is well-known to have a unique solution [4].

In frame of DSM an approximate solution of the scattering problem is constructed as a finite linear combination of the field of dipoles and multipoles deposited in a supplementary domain. Under these conditions the representation for the approximate solution satisfies Maxwell’s equations (1) in  $D_{e,i}$  and the radiation condition (3). The unknown amplitudes of DS are to be determined from the boundary conditions (2). So the boundary value scattering problem under investigation is reduced to the solution of an approximation problem enforced at the obstacle surface  $\partial D$ . One of the most attractive features of DSM consists in the flexible choice of DS fields that can be used for approximate solution construction, which should provide fulfilling Maxwell equations, radiation conditions and yield a complete system of DS fields at the obstacle surface [5]. It is also possible to choose a support of DS, but there some problems can appear. For elongated obstacles as a DS support usually the part of the axis of symmetry is used, but in the case of flat obstacles sometimes there is not enough space for sources deposition. Therefore it can be necessary to find a special support of DS. One of the possibilities is to deposit DS in a complex plane [5]. Such procedure allows to limit a sequence of DS when number of sources  $N \rightarrow \infty$ . This limitation is very important to provide the stability of the numerical model based on DSM.

We will consider an axial symmetric particle. The algorithm of approximate solution construction has some differences for elongated and flat particles, that is why we will separate those two cases. In case of an elongated particle the system of lowest order multipoles distributed on the axis of symmetry  $z$  can be applied to construct an approximation solution [6]. In case of a flat particle we have to use the system of multipoles situated in the complex plane.

Let us shortly describe the procedure of construction of an analytic continuation of DS support to the complex plane with respect to the source’s coordinate  $z_n$ . We will take a halfplane

$$\varphi = \text{const} : \Phi = \{\eta = (\rho, z) \mid \rho \geq 0, z \in R^1\}$$

and a complex plane

$$\tilde{\Phi} = \{\zeta = (\text{Re } \tilde{\zeta}, \text{Im } \tilde{\zeta}) \mid \text{Re } \tilde{\zeta}, \text{Im } \tilde{\zeta} \in R^1\}.$$

Assume the  $\tilde{\Phi}$  match the real axis in such a way that  $\text{Re } \tilde{\zeta}$  coincides with  $z$ . Now we can represent the system of DS functions using the analytical continuation as follows

$$Y_{nm}(x) = h_m^2(k_e, R_{\eta\tilde{\zeta}}) P_m^m(\cos \tilde{\theta}_{\zeta}) \{1, \cos m\varphi, \sin m\varphi\}, \quad n, m \in \mathbf{N}. \tag{4}$$

Where

$$R_{\eta\tilde{\zeta}} = \rho^2 + (z - \tilde{\zeta})^2, \quad \sin \tilde{\theta} = \frac{\rho}{R_{\eta\tilde{\zeta}}}, \quad \cos \tilde{\theta} = \frac{z - \tilde{\zeta}}{R_{\eta\tilde{\zeta}}}.$$

Here  $R_{\eta\tilde{\zeta}}$  is a function of the complex variable  $\tilde{\zeta}$  and it is chosen so that it represents a branch corresponding to the arithmetical root at the positive part of the real axis.

By definition, the point  $\tilde{\zeta} \in \tilde{\Phi}$  is called image of the point  $\eta \in \Phi$  if  $R_{\eta\tilde{\zeta}} = 0$ .

**Lemma 1.** For every point  $\eta = (\rho, z) \in \Phi$  there are 2 images  $\tilde{\xi}^{1,2}$  :

$$\operatorname{Re} \tilde{\xi}^{1,2} = z \quad \text{and} \quad \operatorname{Im} \tilde{\xi}^{1,2} = \pm \rho. \tag{5}$$

**Proof.** The condition  $R_{\eta \tilde{\xi}} \sim = 0$  means that

$$R_{\eta \tilde{\xi}} \sim = (\rho - \operatorname{Im} \tilde{\xi})(\rho + \operatorname{Im} \tilde{\xi}) - 2jm \operatorname{Im} \tilde{\xi}(z - \operatorname{Re} \tilde{\xi}) + (z - \operatorname{Re} \tilde{\xi})^2 = 0,$$

from the last follows (5).  $\square$

**Lemma 2.** Let  $\eta = (\rho, z)$  localized outside or on the surface  $\partial D_i$ . Then the area of corresponding analytical continuation is a coherent area  $D_{\tilde{\xi}} \subset \tilde{\Phi}$ , whose boundary coincides with the generatrix of revolution  $\subset \tilde{\Phi}$ .

**Proof.** The boundary of  $D_{\tilde{\xi}}$  is defined by position of  $\eta$  at the object surface. That means that the singularities are distributed in accordance to (5). Those singularities bound the coherent area at the complex plane  $\tilde{\Phi}$ , whose boundaries coincides with the image of the generatrix . It can be shown that  $\operatorname{Re} R_{\eta \tilde{\xi}} \geq 0$  for every  $\eta$  is localized outside or on the objects surface and  $\tilde{\xi} \in D_{\tilde{\xi}}$  [5].  $\square$

**Notation 1.** The area where  $R_{\eta \tilde{\xi}} \sim$  is an analytical function is symmetric corresponding to the symmetry axis of the scatterer in  $\tilde{\eta}_{\tilde{\xi}}$  according to the Schwarz principle.

**Lemma 3.** Every point  $\tilde{\xi}$  in the complex plane  $\tilde{\Phi}$  generates a circle of singularities in the real space  $\mathbf{R}^3$ .

**Proof.** Let us put  $\tilde{\xi} \in \tilde{\Phi}$ . Then (5) provides us a singularity point  $\eta = (\rho, z)$ , corresponding (5)

$$\rho = |\operatorname{Im} \tilde{\xi}| \quad \text{and} \quad z = \operatorname{Re} \tilde{\xi}. \tag{6}$$

Eq. (6) means that we have singularities distributed on a circle of radius  $\rho$  in  $\mathbf{R}^3$ .  $\square$

**Lemma 4.** Functions (6) with DS situated in  $D_{\tilde{\xi}}$  satisfy Maxwell's equations outside the obstacle and radiation conditions at infinity (3).

**Proof.** Proof is a result of Lemma 1 and the asymptotic of spherical Hankel function.  $\square$

**Theorem.** Let complex coordinates of DS amplitudes  $\{\tilde{\xi}\}_{n=1}^{\infty} \in D_{\tilde{\xi}}$  be distributed in accordance with Notation 1 and have at least one condensing point inside  $D_{\tilde{\xi}}$ , then system (4) is complete and closed in  $L^2(\partial D_i)$ .

We will construct the approximate solution by taking into account not only the rotational symmetry of the obstacle, but also the polarization of an external excitation as well.

In case of a P-polarized exciting plane wave the exciting field accepts the following form

$$\begin{aligned} \mathbf{E}^0 &= (\mathbf{e}_x \cos \theta_0 + \mathbf{e}_z \sin \theta_0)\gamma, \\ \mathbf{H}^0 &= (-\mathbf{e}_y \gamma \cos \theta_0) \sqrt{\epsilon_e \mu_e}, \\ \gamma &= \exp\{-jk_e(x \sin \theta_0 - z \cos \theta_0)\}; \end{aligned} \tag{7}$$

where  $k_e = k \sqrt{\epsilon_e \mu_e}$ .

To take the polarization of the external excitation into account we use a linear combination of electric and magnetic multipoles  $\{w\}_{n=1}^{\infty}$  distributed over the complex plane. For this we need special vector potentials. In case of P-polarization of the plane wave the representation for corresponding vector potentials in a cylindrical coordinate system can be represented as

$$\begin{aligned} \mathbf{A}_{mm}^{1,e,i} &= \{Y_m^{e,i}(\eta, w_n^{e,i}) \cos(m+1)\phi; -Y_m^{e,i}(\eta, w_n^{e,i}) \sin(m+1)\phi; 0\}, \\ \mathbf{A}_{mm}^{2,e,i} &= \{Y_m^{e,i}(\eta, w_n^{e,i}) \sin(m+1)\phi; Y_m^{e,i}(\eta, w_n^{e,i}) \cos(m+1)\phi; 0\}. \end{aligned}$$

Vector potentials for vertical dipoles, which are required to provide completeness of the multipoles's system are

$$\mathbf{A}_n^{3,e,i} = \{0, 0, Y_0^{e,i}(\eta, w_n^{e,i})\}.$$

The representation for vector potentials in case of an elongated particle can be found in [9].

So, the approximate solution taking into account P-polarization of the exciting plane wave and axial symmetry of the particle, can be represented in the form

$$\begin{aligned} \begin{pmatrix} \mathbf{E}_{e,i}^N \\ \mathbf{H}_{e,i}^N \end{pmatrix} &= \sum_{m=0}^M \sum_{n=1}^{N_{e,i}^m} \{p_{mm}^{e,i} \mathbf{D}_1 \mathbf{A}_{mm}^{1,e,i} + q_{mm}^{e,i} \mathbf{D}_2 \mathbf{A}_{mm}^{2,e,i}\} + \sum_{n=1}^{N_{e,i}^0} r_n^{e,i} \mathbf{D}_1 \mathbf{A}_n^{1,e,i}, \quad (8) \\ \mathbf{D}_1 &= \begin{pmatrix} \frac{j}{k\epsilon_{e,i}\mu_{e,i}} \nabla \times \nabla \\ -\frac{1}{\mu_{e,i}} \nabla \end{pmatrix}, \quad \mathbf{D}_2 = \begin{pmatrix} \frac{1}{\epsilon_{e,i}} \nabla \\ \frac{j}{k\epsilon_{e,i}\mu_{e,i}} \nabla \times \nabla \end{pmatrix}. \end{aligned}$$

To provide the convergence of the approximate solution (8) to the exact one it is enough to assure the completeness of the system of distributed multipoles which are used for approximate solutions representation. The scattering from the S-polarized plane wave can be analyzed in the same manner [7].

Now we shortly describe the numerical scheme based on the theory presented above. The approximate solution satisfies Maxwell's equations and radiating conditions at infinity. As the discrete sources are distributed over the symmetry axis of the particle, the approximate solution is a finite linear combination of Fourier harmonics with respect to the  $\varphi$  variable. The exciting plane wave can also be resolved into a Fourier series with respect to the angle  $\varphi$  [7]. As the approximate solution satisfies all the conditions of the original scattering problem, except the boundary conditions, the unknown vector of amplitudes of DS

$$\mathbf{p}_m = \{p_{mm}^{e,i}, q_{mm}^{e,i}, r_n^{e,i}\}_{n=1}^{N_{e,i}^m},$$

where  $p_{mm}^{e,i}$  are amplitudes of electric,  $q_{mm}^{e,i}$ —magnetic and  $r_n^{e,i}$ —vector dipoles in representations [8], is to be determined from the boundary conditions (2). Taking into account the dependence of the incident plane wave on the  $\varphi$  angle, we can reduce the surface approximation problem enforced at the particle surface into a sequence of one-dimensional problems at the particle generatrix. To solve this problem we will use the general matching-point technique [8]. First we choose matching points  $\{\eta_l\}_{l=1}^L$  distributed homogeneously over. Then by matching the representation for the approximate solution and external excitation at the set of matching points and using the axial symmetry we pass from the surface approximation to the approximation for each Fourier harmonic. As a consequence the unknown vector of amplitudes  $\mathbf{p}_m$  can be found as a

pseudosolution of a over-determined system of linear equations

$$\mathbf{B}_m \mathbf{p}_m = \mathbf{q}_m, \quad m = 0, \dots, M.$$

Here  $\mathbf{B}_m$  is a rectangular matrix,  $\mathbf{B}_m = [B_{ij}^m]$ ,  $l = 1, \dots, 4L$ ,  $i = 1, \dots, 2(N_i^m + N_e^m)$ . The reasonable ratio of matching points and number of DS was established as  $2 < L/(N_i^m + N_e^m) < 4$ , the vector of unknown amplitudes  $\mathbf{p}_m$  has length  $2(N_i^m + N_e^m)$  and the vector in the right-hand side can be represented as a  $4L$  vector in the following form:

$$\mathbf{q}_m = (e_{m+1,l}^{0\tau}, e_{m+1,l}^{0\varphi}, h_{m+1,l}^{0\tau}, h_{m+1,l}^{0\varphi})^T,$$

where  $e_{ml}^{0\tau,\varphi} = e_{ml}^{0\tau,\varphi}(\boldsymbol{\eta})$ ,  $h_{ml}^{0\tau,\varphi} = h_{ml}^{0\tau,\varphi}(\boldsymbol{\eta})$ . The components of the vector, in case of P-polarized plane wave excitation, can be written as

$$e_{m+1}^{0\tau}(\eta) = (-j)^m \alpha \cos \theta_0 [J_m(k_e \rho \sin \theta_0) - J_{m+2}(k_e \rho \sin \theta_0)] + 2j\beta \sin \theta_0 \\ \times J_{m+1}(k_e \rho \sin \theta_0) \exp\{-jk_e z \cos \theta_0\},$$

$$e_{m+1}^{0\varphi}(\eta) = -\cos \theta_0 (-j)^m [J_m(k_e \rho \sin \theta_0) + J_{m+2}(k_e \rho \sin \theta_0)] \exp\{-jk_e z \cos \theta_0\},$$

$$h_{m+1}^{0\tau}(\eta) = -\alpha (-j)^m [J_m(k_e \rho \sin \theta_0) + J_{m+2}(k_e \rho \sin \theta_0)] \exp\{-jk_e z \cos \theta_0\},$$

$$h_{m+1}^{0\varphi}(\eta) = (-j)^m [-J_m(k_e \rho \sin \theta_0) + J_{m+2}(k_e \rho \sin \theta_0)] \exp\{-jk_e z \cos \theta_0\}.$$

In case of a S-polarized exciting wave:

$$e_{m+1}^{0\tau}(\eta) = (-j)^m \alpha [J_m(k_e \rho \sin \theta_0) + J_{m+2}(k_e \rho \sin \theta_0)] \exp\{-jk_e z \cos \theta_0\},$$

$$e_{m+1}^{0\varphi}(\eta) = (-j)^m [J_m(k_e \rho \sin \theta_0) - J_{m+2}(k_e \rho \sin \theta_0)] \exp\{-jk_e z \cos \theta_0\},$$

$$h_{m+1}^{0\tau}(\eta) = (-j)^m \alpha \cos \theta_0 [J_m(k_e \rho \sin \theta_0) - J_{m+2}(k_e \rho \sin \theta_0)] + 2j\beta \sin \theta_0 \\ \times J_{m+1}(k_e \rho \sin \theta_0) \exp\{-jk_e z \cos \theta_0\},$$

$$h_{m+1}^{0\varphi}(\eta) = -\cos \theta_0 (-j)^m [J_m(k_e \rho \sin \theta_0) + J_{m+2}(k_e \rho \sin \theta_0)] \exp\{-jk_e z \cos \theta_0\},$$

where  $(\alpha, 0, \beta)$  is the vector, tangential to the generatrix in point  $\eta$ ,  $(\rho, z)$  is the coordinate of the matching point.

Because Fourier harmonics do not depend on the  $\varphi$  angle, the linear system for both P and S polarization corresponding to vertical electric or magnetic dipoles can be written in the form

$$\mathbf{B}_{-1} \mathbf{p}_{-1} = \mathbf{q}_{-1}.$$

In this case  $\mathbf{B}_{-1}$  has a dimension  $2L \times (N_i^m + N_s^m)$ , the right-hand side vector has length  $2L$ , and the unknown vector of amplitudes has length  $(N_i^m + N_s^m)$ . Then we have

$$e_0^{0\varphi}(\eta) = -[j\alpha \cos \theta_0 J_1(k_s \rho \sin \theta_0) + \beta \sin \theta_0 J_0(k_s \rho \sin \theta_0)] \exp\{-jk_s z \cos \theta_0\},$$

$$h_0^{0\tau}(\eta) = jJ_1(k_s \rho \sin \theta_0) \exp\{-jk_s z \cos \theta_0\}.$$

for P polarization and for S case

$$e_0^{\text{or}}(\eta) = jJ_1(k_s \rho \sin \theta_0) \exp\{-jk_s z \cos \theta_0\},$$

$$h_0^{\text{or}}(\eta) = -[j\alpha \cos \theta_0 J_1(k_s \rho \sin \theta_0) + \beta \sin \theta_0 J_0(k_s \rho \sin \theta_0)] \exp\{-jk_s z \cos \theta_0\}.$$

The main differences of the extended DSM scheme described above to the conventional DSM algorithm [1] consist in following:

1. Different numbers of discrete sources  $N_e^m, N_i^m$  are used for the representation of the scattered field outside and total field inside the particle. The numbers of discrete sources are chosen proportionally to the value of the refractive index of the corresponding media. For the internal domain (higher refractive index  $\sqrt{\varepsilon_i \mu_i} > \sqrt{\varepsilon_e \mu_e}$ ) a higher number of discrete sources than for the scattered field  $N_i^m > N_e^m$  is used. In case of flat particles the DS are situated in the complex plane that allows to limit the sequence of DS when  $N \rightarrow \infty$ .

2. The number of discrete sources depends on the rank of Fourier harmonics  $N_{e,i}^m = N_{e,i}(m)$ . For higher harmonics a lower number of multipoles  $N_{e,i}^{m+1} \leq N_{e,i}^m$  is used. This circumstance enables to acquire a more accurate simulation result, provides a monotone decrease of the surface residual and reduces the computer demands up to 30% for a larger particles compared to the conventional DSM model. Besides, it allows to extend the range of validity of the DSM to particles of larger diameters.

After DS amplitudes  $\{\mathbf{p}_m\}_{m=1}^M$  have been determined, the far field pattern can be computed [4]:

$$\frac{\mathbf{E}(\mathbf{r})}{|\mathbf{E}^0(\mathbf{r})|} = \frac{\exp(-jk_e r)}{r} \mathbf{F}(\theta, \varphi) + o\left(\frac{1}{r}\right), \quad r \rightarrow \infty.$$

The vector  $\mathbf{F}(\theta, \varphi)$  has two components in the far zone:  $\varphi$  and  $\theta$ , so that its components are determined at the unit sphere as

$$\mathbf{F}(\theta, \varphi) = \boldsymbol{\theta} \cdot F_\theta(\theta, \varphi) + \boldsymbol{\varphi} \cdot F_\varphi(\theta, \varphi).$$

Using the asymptotic representation for  $Y_{mm}$  for a P-polarized exciting plane wave, components of the far field pattern accepts the form

$$F_\theta^P(\theta, \varphi) = j \sum_{m=0}^M \cos(m+1)\varphi (j \sin \theta)^m \sum_{n=1}^{N_e^m} \{p_{mn}^e \cos \theta + q_{mn}^e\} G_n + j \sin \theta \sum_{n=1}^{N_e^0} r_n^e G_n,$$

$$F_\varphi^P(\theta, \varphi) = -j \sum_{m=0}^M \sin(m+1)\varphi (j \sin \theta)^m \sum_{n=1}^{N_e^m} \{p_{mn}^e + q_{mn}^e \cos \theta\} G_n,$$

where

$$G_n = \exp\{-jk_e z_n \cos \theta\}. \quad (9)$$

The last term in  $F_\theta^P$  corresponds to vertical dipoles.

For S-polarized excitation the far field components can be written as follows

$$F_{\theta}^S(\theta, \varphi) = j \sum_{m=0}^M \sin(m+1)\varphi(j \sin \theta)^m \sum_{n=1}^{N_e^m} \{p_{mn}^e \cos \theta - q_{mn}^e\} G_n,$$

$$F_{\varphi}^S(\theta, \varphi) = j \sum_{m=0}^M \cos(m+1)\varphi(j \sin \theta)^m \sum_{n=1}^{N_e^m} \{p_{mn}^e - q_{mn}^e \cos \theta\} G_n + j \sin \theta \sum_{n=1}^{N_e^0} r_n^e G_n. \quad (10)$$

Using asymptotic representation for  $Y_{mn}$  the components of the far-field pattern can be calculated as a finite linear combination of elementary functions [5].

### 3. Results

We will mostly study the Differential Scattering Cross-section (DSC), which can be calculated analytically via components of the far-field pattern (9), (10) as follows:

$$DSC^{P,S} = |F_{\theta}^{P,S}(\theta, \varphi)|^2 + |F_{\varphi}^{P,S}(\theta, \varphi)|^2.$$

To demonstrate the capabilities of the renewed DSM concept we will present some computational results. As particle material SiO ( $n = 1.67$ ) and an incidence wavelength of 633 nm are chosen due to a typical laser used in optical particle characterization. For description of the particle we will use such parameters like length  $l$ , diameter  $D$  and aspect ratio is  $l/D$ . In case of elongated particles  $l > D$ , and in case of flat particles  $l < D$ . We mostly concentrate on calculation of P-polarized excitation, as it is commonly used in particle characterization.

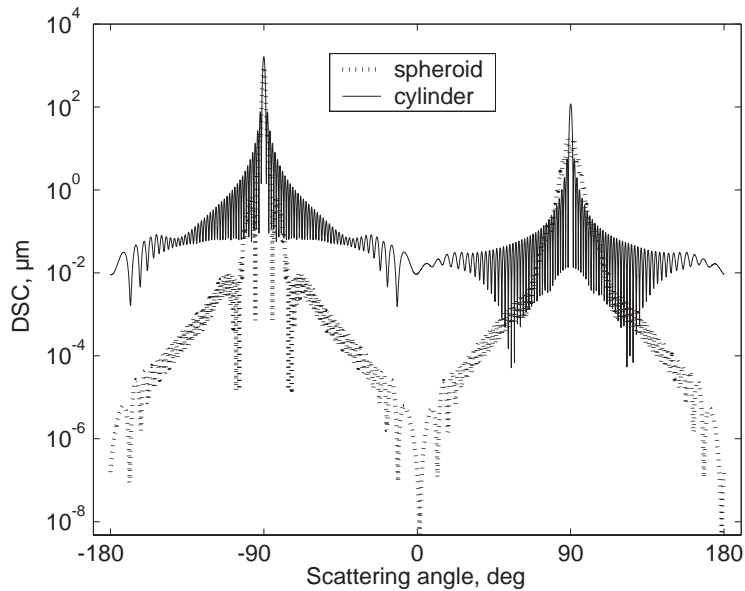


Fig. 1. DSC versus scattering angle for elongated particles with aspect ratio 1:50,  $l = 25 \mu\text{m}$ ,  $D = 0.5 \mu\text{m}$ , under incidence =  $90^\circ$ .

In Figs. 1 and 2 results for elongated particles of different shapes are presented. The results for DSC versus scattering angle for a cylinder and a spheroid of the same parameters are presented in Fig. 1. From comparison, one can see that graphs look different and strongly depend on the shape of particle despite of the same aspect ratio and size. Very interesting is the fact that for the

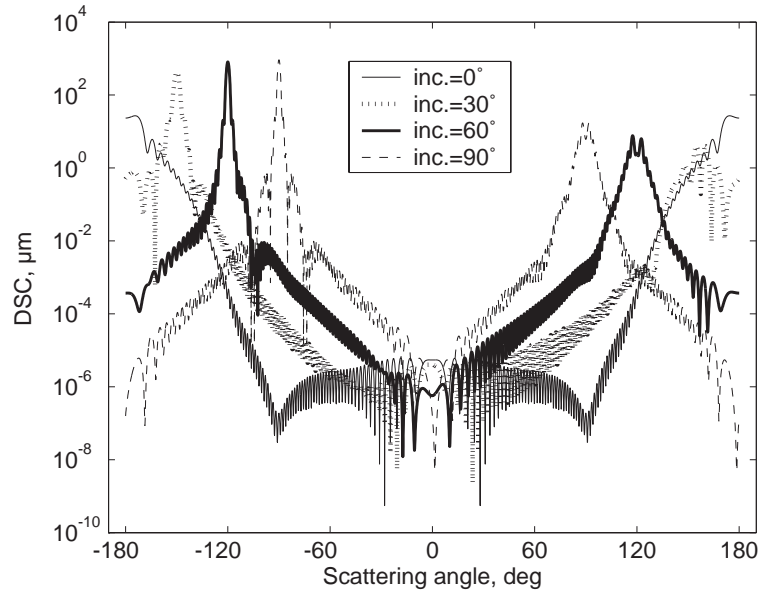


Fig. 2. DSC versus scattering angle for elongated spheroid, with  $l = 25 \mu\text{m}$ ,  $D = 0.5 \mu\text{m}$ , for different incident angles.

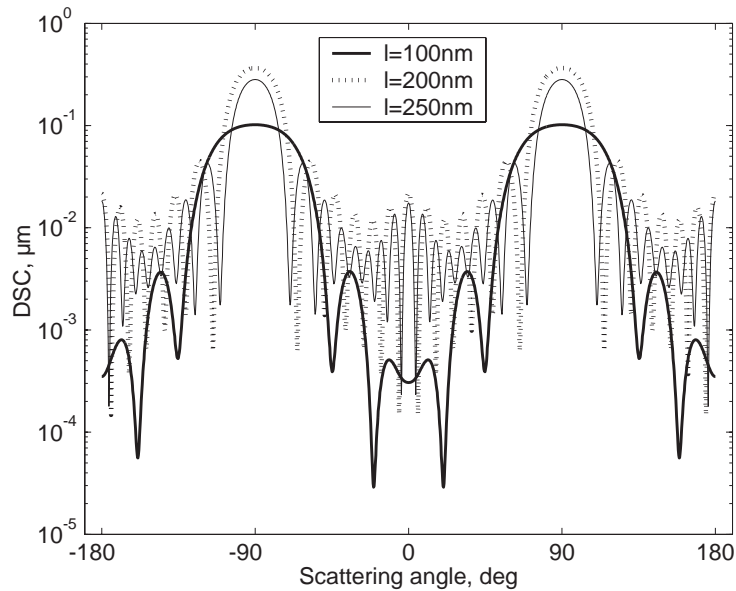


Fig. 3. DSC versus scattering angle for disk-sphere with aspect ratio of 20:1 of different lengths, incidence  $90^\circ$ .

spheroid the back-scattering peak is much smoother and lower than for the cylinder. Fig. 2 presents results for DSC versus scattering angle for a spheroid for different angles of incidence. The results show that the position of main and back-scattering peaks strongly depends on the incident angle while the shape and height of peaks are kept nearly the same.

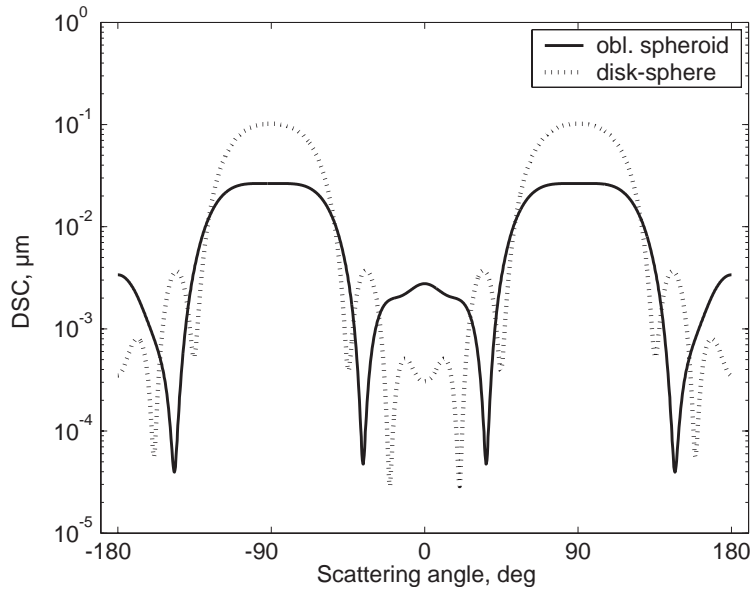


Fig. 4. DSC versus scattering angle for oblate particles with aspect ratio of 20:1,  $D = 0.1 \mu\text{m}$ ,  $l = 2 \mu\text{m}$ , incidence  $90^\circ$ .

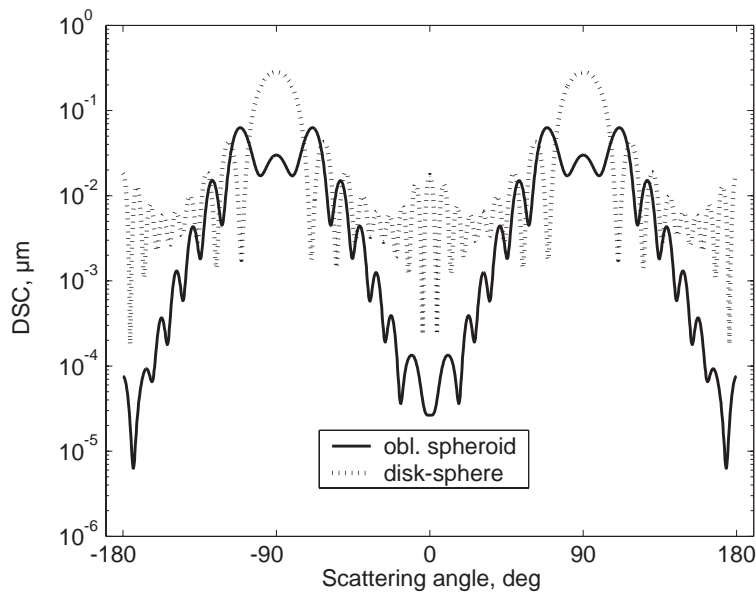


Fig. 5. DSC versus scattering angle for oblate particles of aspect ratio 20:1,  $D = 5 \mu\text{m}$ ,  $l = 0.25 \mu\text{m}$ , incidence  $90^\circ$ .

In Figs. 3–5 results for flat particles are presented. In Fig. 3 results for DSC versus scattering angle for disk-spheres with aspect ratio of 20:1, but different sizes are given. One can see that despite the main features of graphs—positions of main peaks, presence of lower secondary peaks—preserves, the number of peaks and their height are different and that the number of secondary peaks increases together with the dimension of particle. In Figs. 4 and 5 a comparison for different particle shapes is presented. Like in the case of elongated particles the shape also plays the key role for flat particles. Thus, we conclude that both for elongated and for flat particles it is hardly possible to approximate some given shape by some more simple shapes.

#### 4. Conclusion

A renewed effective concept based on DSM is presented in paper. The program code realized using this concept allows to calculate light scattering by particles of extreme shapes. A high aspect ratio of 1:50 for elongated particles and 20:1 for flat particles was achieved. Numerical results presented in this paper show that scattering characteristics essentially depend from particles size and shape. This means that for investigations the choice of a right model used for mathematical modelling plays a key role.

#### Acknowledgements

We would like to acknowledge financial support of this work by Deutsche Forschungsgemeinschaft (DFG).

#### References

- [1] Wriedt T. Generalizes multipole techniques for electromagnetic and light scattering. Amsterdam: Elsevier Science; 1999.
- [2] Sagehorn H, List J, Wiegand T, Weichert R, Wriedt T. Characterization of airborne fibers via Fraunhofer theory: examination of the validity of Fraunhofer theory with the exact scattering theory MMP. Part. Part. Syst. Char. 2001;18(2):55–63.
- [3] Doicu A, Wriedt T. Extended boundary condition method with multipole sources located in the complex plane. Opt Commun 1997;139:85–91.
- [4] Colton D, Kress R. Inverse acoustic and electromagnetic scattering theory. Berlin: Springer; 1992.
- [5] Eremin Y, Orlov N, Sveshnikov A. Models of electromagnetic scattering problems based on discrete sources method. In: Wriedt T, editor. Generalizes multipole techniques for electromagnetic and light scattering. Amsterdam: Elsevier Science; 1999. p. 39–80.
- [6] Eremina E, Eremin Y, Wriedt T. Extension of discrete sources method to light scattering by highly elongate finite cylinders. J Modern Opt 2004;51(3):423–35.
- [7] Doicu A, Eremin Y, Wriedt T. Acoustic and electromagnetic scattering analysis using discrete sources. London: Academic Press; 2000.
- [8] Voevodyn V, Kuznetsov A. Matrices and calculations. Moscow: Science; 1982 [in Russian].
- [9] Eremina E, Wriedt T. Review of light scattering by fiber particles with a high aspect ratio. Recent Res Devel Opt 2003;3:297–318.